**Research**

SHORT COMMUNICATION: ACCELERATED PUBLICATION

# Progress Toward 20% Efficiency in Cu(In,Ga)Se$_2$ Polycrystalline Thin-film Solar Cells

Miguel A. Contreras,[1]* Brian Egaas,[1] K. Ramanathan,[1] J. Hiltner,[2] A. Swartzlander,[1] F. Hasoon[1] and Rommel Noufi[1]

[1]*National Renewable Energy Laboratory, 1617 Cole Boulevard, Golden, CO 80401, USA*
[2]*Colorado State University, Department of Physics, PV Laboratory, Fort Collins, CO 80523, USA*

*This short communication reports on achieving 18·8% total-area conversion efficiency for a ZnO/CdS/Cu(In,Ga)Se$_2$/Mo polycrystalline thin-film solar cell. We also report a 15%-efficient, Cd-free device fabricated via physical vapor deposition methods. The Cd-free cell includes no buffer layer, and it is fabricated by direct deposition of ZnO on the Cu(In,Ga)Se$_2$ thin-film absorber. Both results have been measured at the National Renewable Energy Laboratory under standard reporting conditions (1000 W/m$^2$, 25°C, ASTM E 892 Global). The 18·8% conversion efficiency represents a new record for such devices (Notable Exceptions) and makes the 20% performance level by thin-film polycrystalline materials much closer to reality. We allude to the enhancement in performance of such cells as compared to previous record cells, and we discuss possible and realistic routes to enhance the performance toward the 20% efficiency level. Published in 1999 by John Wiley & Sons, Ltd. This article is a US government work and is in the public domain in the United States.*

## INTRODUCTION

Attaining 20% efficiency by a laboratory-size polycrystalline thin-film (PTF) solar cell is an important indication of the potential to achieve >15% efficiency in commercial PTF modules. For Cu(In,Ga)Se$_2$ (CIGS) thin-film technology, a performance close to 20% will indeed make it equivalent to or even surpass that of current multicrystalline silicon, which already is a commercial product.

Whenever a breakthrough occurs in the field of polycrystalline thin-film solar cells, the first question asked is what is different about the device. Rather than give an extended view on the theories of junction formation in these CIGS-based devices, we will focus on the issues that separate these particular state-of-the-art devices from previous record cells.

* Correspondence to: Miguel A. Contreras, MS 3211, NREL, 1617 Cole Boulevard, Golden, CO 80401, USA.
E-mail: miguel_contreras@nrel.gov

Published in 1999 by John Wiley & Sons, Ltd.

In general, we attribute the enhanced performance to optimized ZnO window layers, an enhanced effective diffusion length of minority carriers, and a reduced recombination in the space-charge region (SCR). The latter benefit stems from an improved interface between the CIGS absorber and the CdS buffer layer.

## EXPERIMENTAL

The main substrate used in these experiments is Mo-coated soda-lime glass; in addition, we have experimented with Mo-coated stainless-steel foils (180 μm thick). The purpose of experimenting with stainless-steel foils is to validate alternative low-cost substrates to the standard soda-lime glass. The CIGS growth process is NREL's patented 3-stage process,[1,2] which incorporates a slight modification in the Ga content and substrate heating profile. Essentially, the Ga content in the first stage (~30% relative to In) is higher than that of the third stage (~25% relative to In). Device fabrication follows by growth of the CdS buffer layer via chemical-bath deposition (CBD) and the ZnO window bilayer grown by RF sputtering. The ~500 Å-thick insulating ZnO is grown from an intrinsic ZnO target, whereas the ~3500 Å-thick conductive layer comes from an $Al_2O_3$-doped ZnO target (2wt%). Cd-free devices skip the CdS deposition step and only use the bilayer ZnO, which is directly deposited on the CIGS absorber. These Cd-free devices use neither 'wet' chemistry nor buffer layers to form the junction. The devices are finished with Ni/Al grids that present a ~5% obscuration loss. All samples incorporate a ~1000 Å-thick antireflection $MgF_2$ coating.

Along with the small area cells ($<1.5$ cm$^2$), we have pursued fabrication of large-area gridded devices (~50 cm$^2$) to explore large-area effects on performance as regarded to interconnecting schemes other than the monolithic interconnection.

## RESULTS AND DISCUSSION

Compositional analysis of absorber layers done by inductively coupled plasma (ICP) spectroscopy reveals the usual Cu-poor characteristics[2] of high-efficiency absorbers and an overall Ga/(In + Ga) of ~0·28. However, an Auger electron spectroscopy (AES) depth-profile analysis indicates a 'normal' graded profile,[2] with higher Ga content in the back of the absorber than in the front (see Figure 1). The expected 'notch,' typical of the 3-stage absorbers, is not as pronounced as with processes where both first and third stages incorporate the same amounts of Ga.
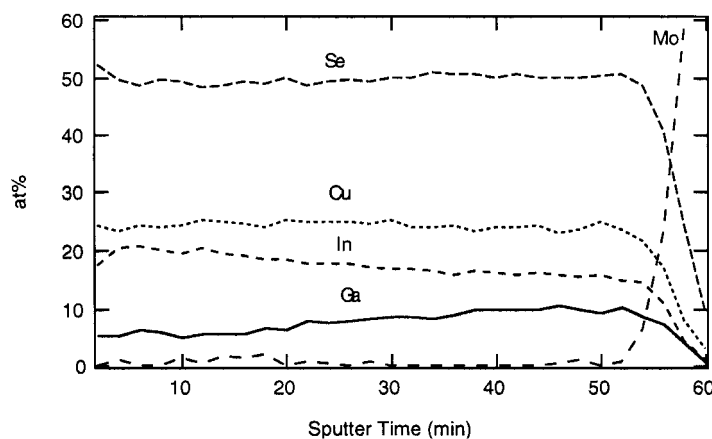


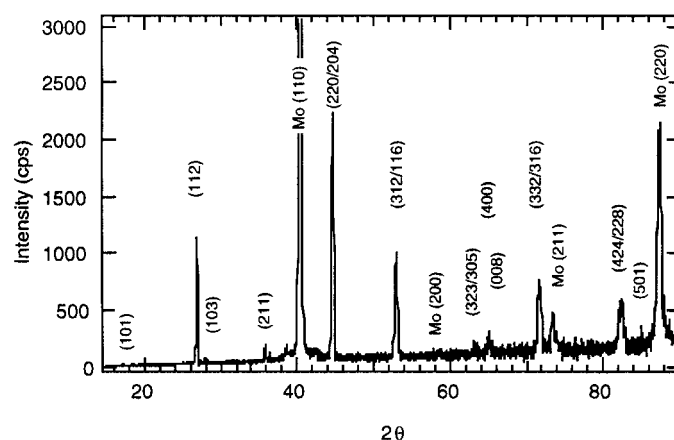Figure 1. Auger depth-profile of CIGS absorber

Figure 2. X-ray diffraction data of CIGS absorber used in record cell. Data taken at room temperature and using the Kα emission from a Cu anode. The higher intensity from the (220/204) reflections indicate possible preferred orientation. This observation has been verified by pole-figure analysis

From a structural point of view, these CIGS absorbers are significantly different from previous ones in that they are characterized by a (220/204) preferred orientation (texture). We have used X-ray pole-figure analysis to determine texture, but this condition can be inferred even from a standard $\theta/2\theta$ scan (see Figure 2). Determination of the exact orientation — either (220) or (204) — is currently being pursued, but the matter is complicated by the fact that the (220) and (204) X-ray reflections overlap for $x \sim 0.3$. However, from a surface point of view, these crystallographic planes are very similar. They show a much more open structure (larger two-dimensional unit cell) than the surface of {112} planes, and they exhibit the lowest polarity of any other crystallographic plane, i.e., they have an equal number of cations and anions.[3] Our previous absorbers (and the ones from other groups[4,5]) have typically been either randomly oriented or, in some cases, (112) oriented. It is not the purpose of this communication to show how a (220/204) texture can be attained — that will be the subject of a separation publication — but we do point out that such a phenomenon strongly depends on substrate type and growth temperature.

The current–voltage (*I–V*) characteristics for the ZnO/CdS/CIGS/Mo and the ZnO/CIGS/Mo record devices are shown in Table I, along with the data from our previous record cell[6] and other selected devices. From Table I, we see at first glance that most of the improvement *apparently* comes from a gain in short-circuit current density ($J_{sc}$) and fill factor (FF). However, we will show later that a more significant gain in open-circuit voltage ($V_{oc}$) has taken place. The relative quantum efficiency (QE) data shown in Figure 3 indeed suggest that the overall collection for the 18·8% cell is superior to the previous record cell.

Table I. Total area *I–V* characteristics of record cells (area includes grid shading). All cells measured under standard reporting conditions (1000 W/m$^2$, 25°C, ASTM E 892 Global). All cells incorporate a MgF$_2$ anti-reflective coating

| Sample ID | Area (cm$^2$) | $V_{oc}$ (mV) | $J_{sc}$ (mA/cm$^2$) | Fill factor (%) | Efficiency (%) | Notes |
|---|---|---|---|---|---|---|
| C1068-2#5 | 0·449 | 678 | 35·22 | 78·65 | 18·8 | ZnO/CdS/CIGS/Mo* |
| S773-B14#6 | 0·414 | 674 | 33·98 | 77·24 | 17·7 | ZnO/CdS/CIGS/Mo* (previous record) |
| C1076-22#2 | 0·462 | 604 | 36·19 | 68·64 | 15·0 | ZnO/CIGS/Mo (Cd-free device) |
| C1099-3#3 | 1·129 | 667 | 36·45 | 74·93 | 18·2 | ZnO/CdS/CIGS/Mo† |
| C1007 | 43·890 | 646 | 31·97 | 66·19 | 13·7 | Large-area cell |
| M1961-14#5 | 0·4138 | 646 | 36·38 | 74·19 | 17·4 | Mo/stainless-steel substrate |

*Notable exception.
†Class record.
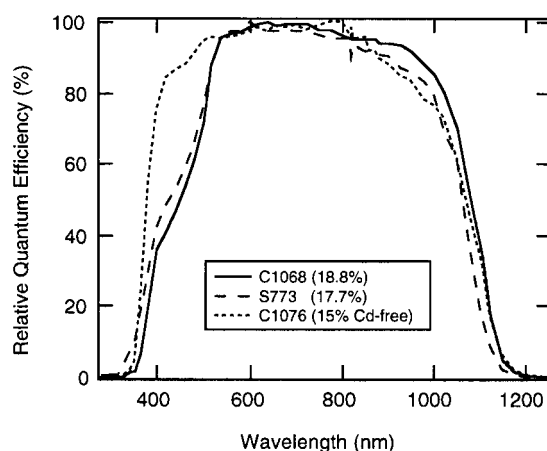
Figure 3. Relative (or normalized) quantum efficiency data for selected devices. Data acquired at 25°C with a light bias of 10 mA (bias voltage = 0). Light bias is accomplished by 'white' light with an intensity level that generates 10 mA of short-circuit current in the cell
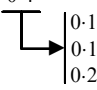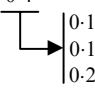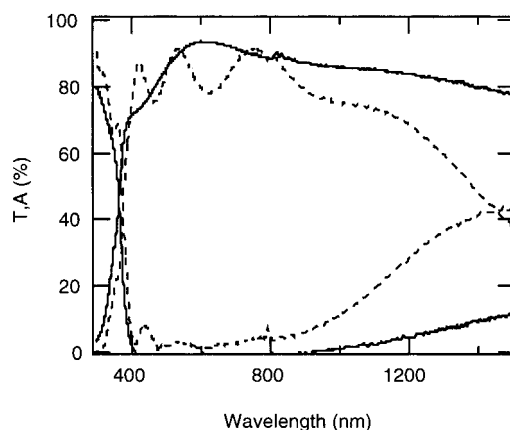


Figure 4. Transmission (top) and absorbance (bottom) data for 'old' ZnO bilayer (dashed lines) and improved bilayer (solid lines)

This gain starts at about 600 nm and continues all the way into the infrared (IR) region. We attribute *part* of this gain in current to optimized ZnO window bilayer and antireflective (AR) coatings. Essentially, the improved ZnO window material shows a higher transmittance (or less absorbance) in that same region of the spectrum. An optical comparison between our 'old' ZnO bilayer and the recently optimized bilayer is shown in Figure 4.

The gain in current in the IR region can also be explained via an enhanced effective-minority carrier diffusion length in the absorber. Junction electron-beam induced current (EBIC) characterization indeed reveals that collection in the record cell extends well within the absorber layer ($\sim$1·5 $\mu$m from the metallurgical junction). It is possible that the built-in electric field created by the 'normal' grading in the absorber functions as a very effective 'back surface field.' On the other hand, the Cd-free device has poor collection in the IR, and the EBIC scans show an extremely narrow collection profile ($<$0·2 $\mu$m wide) centered right at the CIGS/ZnO interface. Such characteristics suggest that the Cd-free cell may be a true heterojunction device (not a buried junction). As expected, collection in the shorter wavelengths ($<$550 nm) is enhanced in this device due to the absence of CdS or other buffer layers.

Table II. Summary of ideal solar cell parameters extracted from room-temperature $I$–$V$ and QE data for a comparison between samples S773-B14#6 and C1068-2#5. $R_s$ is series resistance, $r_{sh}$ is shunt resistance, and $A$ is diode quality factor

| Parameter | S773-B14#6 | C1068-2#5 | Change in efficiency (%) | Adjusted for bandgap |
|---|---|---|---|---|
| Efficiency | 17·7% | 18·8% | 1·1 | 1·1 |
| Bandgap | 1·14 eV | 1·12 eV | – | – |
| $J_{sc}$ | 34·0 (mA/cm²) | 35·2 (mA/cm²) | 0·6 | 0·2 |
| $V_{oc}$ | 674 (mV) | 678 (mV) | 0·1 | 0·5 |
| FF | 77·0% | 78·6% | 0·4 | 0·4 |
| $R_s$ | 0·3 (Ω-cm²) | 0·2 (Ω-cm²) | ⌐ 0·1 | ⌐ 0·1 |
| $r_{sh}$ | 3800 (Ω-cm²) | 10,000 (Ω-cm²) | → 0·1 | → 0·1 |
| $A$ | 1·6 | 1·5 | 0·2 | 0·2 |

The QE data in Figure 3 also show that the effective bandgap of the 18·8% cell (∼1·12 eV) is narrower than that of the previous record cell (∼1·14 eV). Considering the $V_{oc}$ values shown in Table I and the estimated bandgap values, we see that the 18·8% cell achieves a higher voltage from the bandgap as compared to the previous record cell. Because it has been argued that performance in heterojunction solar cells is dominated by recombination in the SCR,[7] we suggest that the gains in voltage and fill factor are very likely a result of a reduced SCR recombination.

To render more validity to the above arguments (reduced SCR recombination), we have applied the ideal solar cell model to the 18·8% and the 17·7% record cells. Because such cells behave very well from the point of view of the ideal model (good fit to $I$–$V$ curves), the cell parameters extracted from such analysis can be used to compare the cells and to detail more quantitatively where the gains come from. The summary of this analysis is shown in Table II. From Table II, we see again that a significant improvement comes from a better FF value. However, when bandgap arguments are taken into account, a great deal of the improvement can be associated to the $V_{oc}$ and, to a lesser degree, to the gain in current. The lower diode quality factor *(A)* of the 18·8% cell indeed attests to a much-improved junction and, therefore, a reduced SCR recombination.

Because recombination centers can be associated with defects in the SCR, we consider as a thesis that the 'new' interface between the (220/204) oriented CIGS thin film and the CdS buffer layer — and/or the ordered defect compound[8] (ODC) — results in a lower density of crystallographic imperfections. Structural questions still remain about how the ODC (if any) grows on the surface of these (220/204) textured absorbers.

For certain CBD growth conditions, CdS has been reported to grow epitaxially with cubic structural phase on {112} CIGS surfaces.[9] Nevertheless, the reported {111}$_{cubicCdS}$//{112}$_{CIGS}$ epitaxial relationship is not free of defects; in fact, stacking faults have been observed in similar CdS layers.[10] In any event, because these {220/204} CIGS surfaces are characterized with a much more open structure as compared to {112} surfaces, impurity diffusion can be expected to be enhanced. Of particular interest is additional facilitation of Cd (or Zn) diffusion into the CIGS and different possibilities for the proposed Cu–Cd ion exchange[11] at this interface.

To further enhance performance toward the 20% level, we suggest that similar issues to the ones discussed above must be pursued: (1) Further optimizations of the window materials, and perhaps even the replacement of ZnO by other similarly conductive, yet more transparent, conductive oxide materials — for instance, cadmium stannate[12] ($Cd_2SnO_4$); (2) Optimizations of AR coatings by fabrication of bilayer structures, as is done in other related technologies (total QE data suggest that there are still significant losses due to reflection); (3) Widening the bandgap of CdS via alloying, i.e., (Cd,Zn)S or other suitable materials, to allow more photons to reach the junction; and (4) Slight bandgap enhancement or bandgap engineering of the absorber in order to boost $V_{oc}$ and FF values but preserve short-circuit current. At these levels of performance, structural and electrical aspects of the CIGS/ODC and ODC/CdS

interfaces[13,14] become more relevant, and they may provide additional routes to enhance performance in CIGS-based solar cells.

As a final comment, we conclude that preferred orientation in the absorber is not a necessary condition for attaining high efficiency in ZnO/CdS/CIGS/Mo structures — as evidenced by the fact that high performance ($>15\%$) has been attained with randomly oriented films, (112) oriented films, and now, (220/204) textured films. However, the issue of texture may be more relevant for Cd-free structures, which rely on direct ZnO deposition onto the absorber. Further work needs to be performed on surfaces and interfaces of CdS/CIGS structures, with particular attention to structural and electrical aspects of such interfaces.

*Acknowledgements*

# *REFERENCES*

1. U.S. Patent No. 5,441,897 (August 15, 1995) and U.S. Patent No. 5,436,204 (July 25, 1995).
2. M. A. Contreras, J. R. Tuttle, A. Gabor, A. Tennant, K. Ramanathan, S. Asher, A. Franz, J. Keane, L. Wang, J. Scofield and R. Noufi, 'High efficiency Cu(In,Ga)Se$_2$-based solar cells: Processing of novel absorber structures', *Conference Record of the 24th IEEE Photovoltaics Specialists Conference*, Waikoloa, HI, December 1994, pp. 68–75.
3. R. Scheer, 'Surface and interface properties of Cu-chalcopyrite semiconductors and devices', *Trends in Vacuum Science and Technology*, **2**, 77–112 (1997).
4. W. N. Shafarman, R. W. Birkmire, M. Marudachalam, B. E. McCandless and J. M. Schultz, 'Fabrication and characterization of Cu(In,Ga)Se$_2$ solar cells with absorber bandgap from 1·0 to 1·5 eV', *AIP Conference Proceedings 394, NREL/SNL PV Program Review*, Lakewood, CO, November 1996, pp. 123–131.
5. J. Hedström, H. Ohlsén, M. Bodegård, A. Kylner, L. Stolt, D. Hariskos, M. Ruckh and H. W. Schock, 'ZnO/CdS/Cu(In,Ga)Se$_2$ thin film solar cells with improved performance', *Conference Proceedings of the 23rd IEEE Photovoltaic Specialists Conference*, Louisville, KY, May 1993, pp. 364–371.
6. J. R. Tuttle, J. S. Ward, A. Duda, T. A. Berens, M. A. Contreras, K. R. Ramanathan, A. Tennant, J. Keane, E. Colde, K. Emery and R. Noufi, 'The performance of Cu(In,Ga)Se$_2$-based solar cells in conventional and concentrator applications', *Conference Record, 1996 Spring Materials Research Society*, San Francisco, CA, April, Vol. 426, 1996, pp. 143–152.
7. A. L. Fahrenbruch and R. H. Bube, *Fundamentals of Solar Cells*, Academic Press, New York, 1983.
8. D. Schmid, R. Ruckh, F. Grunwald and H. W. Schock, 'Chalcopyrite/defect chalcopyrite heterojunctions on the basis of CuInSe$_2$', *J. Appl. Phys.*, **73**(6), 2902 (1993).
9. T. Nakada, 'Cd-doping into Cu(In,Ga)Se$_2$ thin films by chemical bath deposition process', *Proceedings of the 12th Sunshine Workshop on Thin Film Solar Cells, Technical Digest*, Tokyo, Japan, January 1999, pp. 61–68.
10. M. J. Furlong, D. Lincot, M. Froment, R. Cortes, A. N. Tiwari, M. Krejci and H. Zogg, 'Heteroepitaxial growth of chemical bath deposited CdS on single crystal CuInSe$_2$ substrates', *Conference Proceedings of the 14th European Photovoltaic Solar Energy Conference*, Barcelona, Spain, June 1997, pp. 1291–1294.
11. K. Ramanathan, H. Wiesner, S. Asher, D. Niles, R. Bhattacharya, J. Keane, M. A. Contreras and R. Noufi, 'High-efficiency Cu(In,Ga)Se$_2$ thin film solar cells without intermediate buffer layers', *Conference Proceedings of the 2nd World Conference in Photovoltaic Energy Conversion*, Vienna, Austria, 1998, pp. 477–481.
12. X. Wu, P. Sheldon, T. J. Coutts, D. H. Rose, W. P. Mulligan and H. R. Moutinho, 'CdS/CdTe thin-film devices using a Cd$_2$SnO$_4$ transparent conductive oxide', *Proceedings of the 14th Conference NREL/SNL Photovoltaics Program Review*, Lakewood, CO, November, AIP Conf. Proc. 394, 1996, pp. 693–702.
13. A. Niemegeers, M. Burgelman, R. Herberholz, U. Rau, D. Hariskos and H. W. Schock, 'Model for electronic transport in Cu(In,Ga)Se$_2$ solar cells', *Progress in Photovoltaics: Research and Applications*, **6**(6), 407–421 (1998).
14. M. A. Contreras, H. Wiesner, J. Tuttle, K. Ramanathan and R. Noufi, 'Issues on the chalcopyrite/defect-chalcopyrite junction model for high-efficiency Cu(In,Ga)Se$_2$ solar cells', *Technical Digest of the International PVSEC-9*, Miyazaki, Japan, 1996, pp. 127–130.